Tribology International 160 (2021) 107002

Contents lists available at ScienceDirect

Tribology International

journal homepage: http://www.elsevier.com/locate/triboint

Scuffing evaluation of fully formulated environmentally acceptable lubricant using barrel-on-disc technique

Reza Bayat *, Arto Lehtovaara

Tribology and Machine Elements, Materials Science and Environmental Engineering, Faculty of Engineering and Natural Sciences, P.O. Box 589, 33014, Tampere University, Tampere, Finland

ARTICLE INFO

Keywords:
Scuffing
Tribofilm
Environmentally acceptable lubricant
Running-in

ABSTRACT

Scuffing evaluation is challenging due to the catastrophic nature of this failure mode. In this paper, a new scuffing test method was designed for evaluating the scuffing capacity of fully formulated industrial oils. A barrel-on-disc technique was employed in which the specimens are moving in opposite direction under rolling–sliding conditions. The maximum Hertzian pressure could reach up to 3.06 GPa, and the test plan was a combination of increasing-sliding speed and increasing-load steps. Furthermore, the tribofilm evolution was captured using Spacer Layer Interferometry Method (SLIM), and the correlation of tribofilm and micro-scuffing/scuffing was presented. Results revealed the difference between the scuffing capacity of Environmentally Acceptable Lubricants and the Mineral oils which had the same scuffing capacity in their datasheet.

1. Introduction

Environmental considerations force the industries to use Environmentally Acceptable Lubricant (EAL) in locations that there is the risk of environmental pollution. The formulation of these oils is still under development, and it is required to understand their performance difference from conventional mineral oil. One of their differences is their scuffing capacity. Scuffing is a failure recognized by high wear rate and roughened surface, increased temperature and friction, and generated noise and vibration [1]. Compared to other tribological failure types like mild wear and fatigue, scuffing is hard to predict and study because of its catastrophic nature. Savolainen and Lehtovaara showed that even a short overload period can initiate the scuffing [2]. Therefore, choosing the right scuffing test is highly important to prevent misinterpretation of scuffing results.

In order for scuffing to occur, the elasto-hydrodynamic (EHL) film and protective tribofilm must be broken [3], and plastic yielding happens in the sliding surfaces [4]. The collapse of the EHL film is attributed to frictional heat generation [5–8], high lubricant starvation due to accumulated wear products [9], lubricant degradation [10], wettability and roughness of surface [11] and high shear stress [12]. The tribofilm breakdown is related to the desorption of reacted polar molecules generated by EP additive [13]. However, understanding these factors has not resulted in a single accepted theory for the scuffing. The flash temperature hypothesis was amongst the first scuffing theories, suggesting that scuffing occurs when the contact temperature within the central region of the contact reaches a critical value for a given lubricant/surface combination [14]. This theory did not consider the effect of EHL film collapse, thus Dyson proposed a model describing that the critical temperature occurs in the inlet of contact [15]. Cheng and Dyson later added to the theory by considering the effect of asperity heating [16]. More recent theories focus on the evolution of the metallic contact according to the adiabatic shear plastic instability in the near-surface material [17–21]. Ajayi et al. observed a sudden temperature rise in the contact and concluded that it is contrary to the critical temperature theory for scuffing initiation. Ajayi et al. suggested that the sudden temperature rise is the result of scuffing, not its causality [18]. It is noteworthy that examining scuffing theories is not the aim of this paper. These theories were remarked since they are used for explaining the experimental results in the current study.

Scuffing has been studied using different experimental techniques such as Ryder [22], IAE [23], FZG [24,25], Timken [26], four-ball [27] and twin-disc [2,28]. Peng et al. discussed the problems with these methods and divide the causes into two main categories: stationary body, and conventional increasing-load test sequences [29]. The stationary body in four-ball and Timken tests suffers from cumulative wear before scuffing. This wear increases the contact area and reduces the contact pressure. This geometrical transformation can lead to wrong oil ranking in case of testing a low wear capacity oil [29]. One solution for avoiding this problem is using rolling-sliding contact that distributes the wear over the surface and prevents high wear on a single point. Thus, employing tests like Ryder, IAE, FZG are preferred regarding the wear issue. However, in these methods, the increasing-load sequences bring

* Corresponding author.
E-mail address: reza.bayat@tuni.fi (R. Bayat).

https://doi.org/10.1016/j.triboint.2021.107002
Received 11 January 2021; Received in revised form 24 February 2021; Accepted 15 March 2021
Available online 19 March 2021

the unworn fresh asperities in contact at the start of each load step. Thus, the risk of premature scuffing is increased due to the contact of unprotected asperities. In addition, another problem with both conventional rolling-sliding and pure sliding tests is that the sliding speed can not be increased without increasing the rolling speed. Consequently, with increasing the sliding speed the rolling speeds will be higher resulting in the entrainment of more lubricant into the contact and formation of a thick EHL film [29]. To avoid such problems, Ingram et al. employed a ball-on-disc machine to provide a rolling-sliding contact in contra-rotation mode [30]. This technique provided low oil entrainment speed and decoupling of sliding and rolling speeds that allowed performing the scuffing test with increasing-sliding-speed sequences instead of increasing-load sequences. That contra-rotating ball-on-disc method was further improved by Peng et al. aiming for higher repeatability and scuffing prediction [29]. However, the increasing-sliding speed sequences used in these studies fail to differentiate between the performance of various oils with low to high scuffing capacity range.

Real component tests like FZG are critical to examine the performance of a lubricant. Unfortunately, these tests are costly and time-intense. Therefore, laboratory tests can be used for the primary screening and grasping scientifically analyzed results that apply to the real components. Using a fully formulated lubricant is necessary for these prior laboratory tests since the results can be correlated to the real component tests. Considering this fact, these industrial oils have been commonly used in scientific papers as well [31–35]. This paper aims to modify the contra-rotating method for evaluating the scuffing capacity of fully formulated environmentally acceptable lubricant. The modification of the test sequences minimizes the error and captures big or small scuffing capacity differences between the oils. Achieving this goal, the ball specimen is replaced with a barrel specimen to generate high Hertzian pressure. Although using the barrel-on-disc method is not conventional for scuffing test, it has been used for studying micropitting [36], surface/lubricant interactions [37] and white etching cracks [38]. In addition, the spacer layer imaging method (SLIM) is used to capture the tribofilm evolution and illustrate the tribofilm/lubricant interaction during different stages of the scuffing test.

2. Experiment detail

2.1. Experimental rig

The scuffing tests were performed using the barrel-on-disc technique provided by a mini-traction machine (MTM). Fig. 1 shows a schematic view of the test rig and barrel/disc specimens. The barrel and disc are in rolling sliding contact, and the friction force is measured by a load cell mounted between the barrel shaft and the instrument body. The barrel shaft is tilted to minimize the spin, and it is rotating independently from the disc shaft to provide a wide range of rolling and sliding speeds. Rolling speed denotes the lubricant entrainment speed, and sliding speed has a direct relation to the shear stress and heat generation. For this rolling/sliding contact, these speeds are expressed by Eqs. (1) and (2):

$$U_e = \frac{U_d + U_b}{2} \tag{1}$$

$$U_s = U_d - U_b \tag{2}$$

where U_d and U_b are respectively the disc and barrel velocities in the contact point, U_e is the entrainment velocity and U_s is the sliding velocity.

During the tests, the pot and lubricant temperatures were monitored by two separate sensors, one mounted in the pot and another in contact with the lubricant. Adjusting the right temperature, a heater generates the required amount of heat, and the cooler transfers the excessive heat.

Picturing the tribofilm thickness evolution is a key factor in understanding the scuffing mechanism. The stress imposed on the surface and asperities is influenced by the liquid lubricant film, and tribofilm thickness and properties [39]. To achieve this goal, the spacer layer imaging method (SLIM) was used. In this technique, the barrel is uploaded against a spacer layer of transparent silicon dioxide coated with a thin, semireflective layer of chromium. Then, a white light beam is shone into the contact between the specimen and the spacer layer that proves a colored interference image. This image is recorded by the camera shown in Fig. 1 (a). By capturing this image at different intervals, the tribofilm thickness changes can be studied [40].

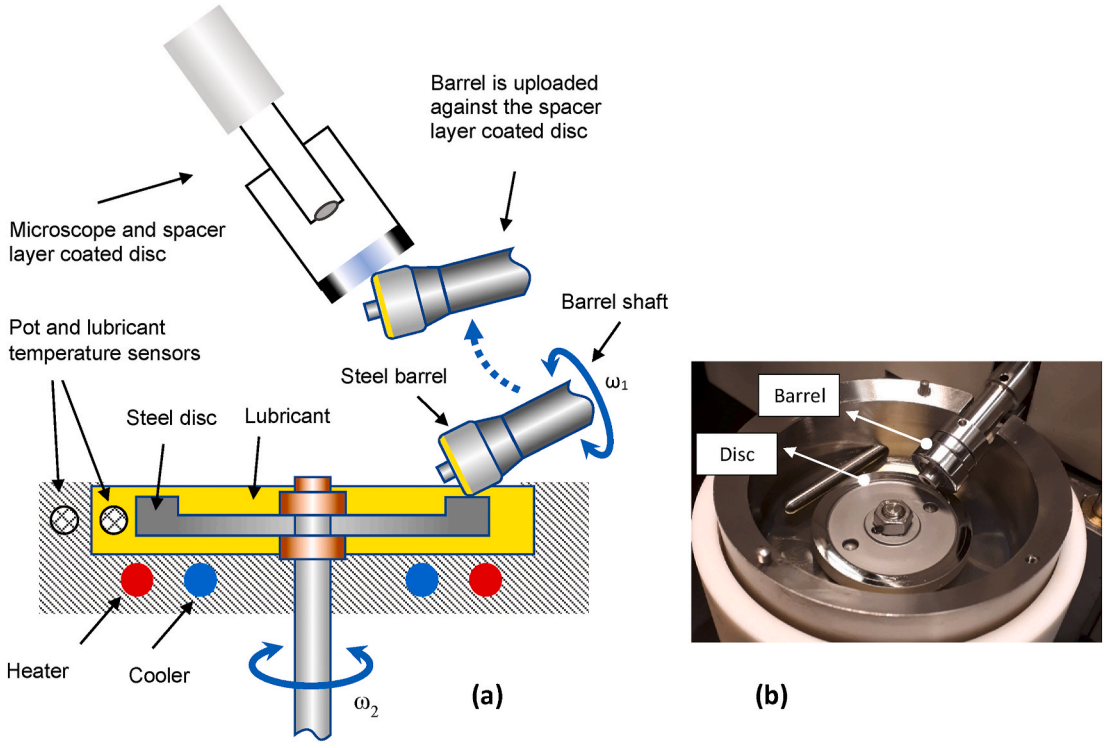

Fig. 1. Barrel on disc test: (a) schematic of MTM with barrel on disc samples (b) an image of the test samples.

2.2. Test specimen

The barrel's diameter was 19.05 mm, and the edge a fillet with 2 mm diameter that was in the contact with a rotating flat disc (Fig. 1). The barrel and disc specimens were both AISI 52100 steel with a hardness of 750–770 H V, elastic modulus of 207 GPa and surface roughness indicated in Table 1, where S_a is the average roughness height of area, and S_q is Root-Mean-Square roughness height of area. For each scuffing test, a fresh barrel and disc were used those were cleaned by immersion in toluene and isopropanol in an ultrasonic bath for 10 min. The roughness parameters and the surface profile were measured by an Alicona InfiniteFocus G5 optical profilometry system. The roughness was measured at three locations with an area of 887 × 252 μm^2. The cut-off was 250 μm, and the filter was a Gaussian filter for inclined planar surfaces (ISO 16610–61).

2.3. Tested lubricants

Comparing the scuffing capacity of the environmentally acceptable lubricants, two different EALs with the same viscosity were selected. These two EAL oils meet the US EPA regulations for "Environmentally Acceptable Lubricants", accordingly they demonstrate the VGP requirements for biodegradability, toxicity, and bioaccumulation. For the reference oils, two mineral oils were selected. One of these mineral oils was gear oil from the same viscosity class, and the other one was an engine oil that had a similar 40 °C kinematic viscosity. Except for the case of M1, all the oils have an FZG scuffing capacity of 12+ according to the manufacturer datasheet, and comply with the DIN 51517 part 3 (CLP) standard. The details of oil's properties, and additives elemental composition can be found respectively in Table 2 and Table 3:

2.4. Selecting the test parameters

A scuffing test method for a ball-on-disc test rig has been developed in Refs. [29,30] based on the contra-rotation scuffing test approach. In that contra-rotation scuffing test, the sliding speed increases in scuffing steps while the load and entrainment speed are constant. This criterion is contrary to the conventional scuffing tests in which the increasing-load steps are used. This sliding step criterion [29,30] was designed to avoid the conventional scuffing test problems discussed in section 1. In this paper, the test method is similar to the sliding-step criteria, however, some adjustments are done for testing the high scuffing capacity of fully formulated oils.

The first adjustment is about the running-in stage. It is widely accepted that the surface roughness parameters and distribution of asperity heights are very determinative in the scuffing of machine elements [39]. In addition, running-in not only changes the surface roughness and geometry, it changes the undersurface material properties [17]. One source of high variation in scuffing results is the difference between the micro-topography of every two surfaces. Ingram et al. suggested using the actual test load with very low sliding and entrainment speeds for the running-in stage [30]. Peng et al. observed that a running-in with the actual test load results in considerable damage on the surfaces, and recommended using lower loads to polish the high asperities at the middle of contact [29]. In this paper, a similar low load, low sliding speed running-in test with a duration of 600 s was employed. However, after several experiments with this condition, premature scuffing was observed which means unexpected scuffing at low sliding speeds. To prevent this, an extra short running-in stage was added to the test plan with the same load. These extra running-in periods are performed with the same load as the test, and with lower sliding speed (red points in Fig. 2 denote running-in).

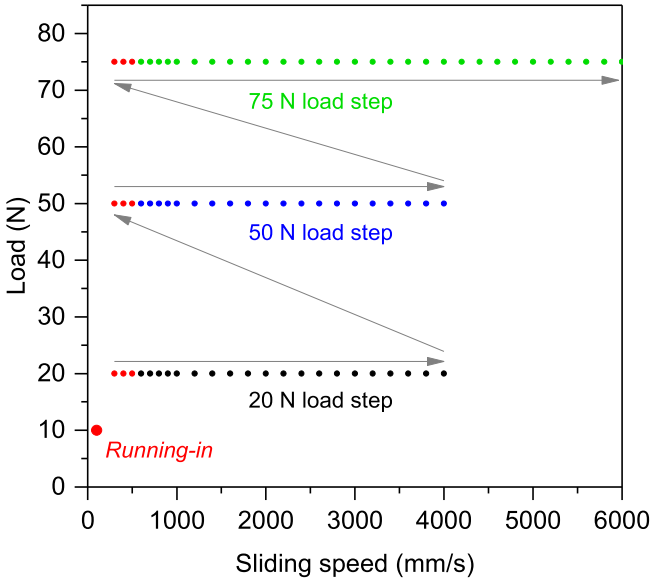

Fig. 2. The variation of the load and sliding speed of the developed scuffing test. The duration for each test point is 30 s, and there is a rest stage of 30 s between each point.

Table 1
Barrel and disc average roughness parameters.

Specimen	Sa (nm)	Sq (nm)
Barrel	90	114
Disc	92	118

Table 2
Measured lubricants properties.

	Kin. Vis. @40 °C (cSt)	Kin. Vis. @100 °C (cSt)	ρ @15 °C (kg/m^3)	VI	Comment
Method	ASTM D445	ASTM D445	EN ISO 12185	ASTM D2270	
M1	127.60	13.83	908	105	Mineral engine oil SAE 40
M2	142.50	14.24	888	97	Mineral gear oil ISO VG 150
EAL1	147.50	18.84	972	145	Synthetic gear oil, Group V, EAL ISO VG 150
EAL2	150.57	18.44	929	137	Synthetic gear oil, Group V, EAL ISO VG 150

Table 3
Elemental analysis of additives in oils according to ASTM D5185.

	Calcium	Magnesium	Boron	Zinc	Phosphorus	Barium	Sulphur
M1	13822	37	1	399	330	0	4704
M2	0	0	36	0	358	0	8391
EAL1	0	0	1	0	864	0	951
EAL2	1	0	0	1	752	0	2080

The second adjustment was about the load in the scuffing test. After tuning the running-in parameters, the first tests were carried out using 20 N load (1.97 GPa) to observe the oils scuffing behavior. With a constant 20 N load, the sliding speed was increased in small steps (Fig. 2 and Table 4). At this load, the mineral oils were showing scuffing, however, no scuffing was observed for the EALs even with sliding velocities of 7000 mm/s. It appeared that the developed sliding speed-step criteria in Refs. [29,30] is not efficient for comparing the oils with a big scuffing capacity difference.

For the case of EALs, after the test with 20 N load, the load was increased by 5 N in several intermediate steps till 75 N that is the limit for the machine (similar to Fig. 2, but with more intermediate load steps). No success was observed with this action and no scuffing was observed for EALs. This is due to a low maximum pressure on the specimen caused by gradual wear on the surfaces which was observed in SLIM images (similar to Fig. 8). This was showing that increasing the load with small steps leads to wear that postpones wear. The same procedure was repeated with 10 N intervals, but it was observed that again the wear persists and prevents scuffing in the machine operational ranges. However, three load-steps of 20 N (Pmax:1.97 GPa), 50 N (Pmax:2.67 GPa), and then 75 N ((Pmax:3.06 GPa) showed promising results. Furthermore, to prevent the excessive wear, the sliding speed was limited to 4000 mm/s for the load step of 20 N and 50 N.

In the final test plan (Fig. 2), a primary running-in is completed, and then the excessive running-in is performed for the load stage of 20 N. After that, the sliding speed increases from 600 mm/s to 4000 mm/s at a load of 20 N (Pmax:1.97 GPa, Pmean:1.31 GPa). If no scuffing appears, the next series of sliding steps are performed with a load of 50 N (Pmax:2.67 GPa, Pmean:1.79 GPa), and then 75 N ((Pmax:3.06 GPa, Pmean:2.05 GPa). It is noteworthy that before each load step, an excessive running-in (red points in Fig. 2) is considered that has the same load as the load-step. This is for preventing the contact between fresh unprotected asperities. In conclusion, the current test method is a combination of the load-step criteria and sliding speed-step contra-rotation method without their disadvantages. The detail of the parameters is given in Fig. 2 and Table 4.

Each test point in Fig. 2 illustrates a test with constant velocity and load in a 30 s long test. The optimum duration of 30 s was also an optimized number. With a 10 and 20 s duration, scuffing can be postponed to one or more sliding steps because there is not enough time for the temperature rise and adhesion between to surfaces, and with longer than 30 s duration the effect of wear plays an adverse role. After each test point, there is a 30 s rest stage to allow the specimens' bulk temperature to return to the oil temperature [29]. At these rest steps, the SLIM image from the barrel surface is captured.

3. Results and discussion

Using the developed test method, the scuffing capacity was assessed for the oils listed in Table 2. This approach compares the scuffing capacity of the oils through a recorded friction-time and PV graph. Three repeats were done for each oil to have an estimation of the test error.

3.1. Ranking the oils scuffing capacity

Fig. 3 shows the recorded friction coefficient of the tested oils during the test stages neglecting the rest stage time. Scuffing was recognized by a rapid and unrecoverable increase in friction coefficient to over 0.2. This friction jump was accompanied by a significant increase in test noise and rig vibrations. In Fig. 3, a clear difference is visible between the oils' scuffing performance. EALs showed better performance compared to the mineral oils, and EAL1 was the best and M1 was ranked the worst oils. Matveevsky suggests that the scuffing risk is related to Friction Power Intensity which is the product of the coefficient of friction before scuffing, mean contact pressure, and sliding speed (FPI = μPUs) [41]. This criterion has been used for predicting the onset of scuffing [16], and it is effective to distinguish between oils with different scuffing performances [29]. Fig. 4 shows FPI at scuffing plotted against mean contact pressure for the tests. A clear difference can be observed between the FPI value of the oils with the mean value of 124 MW/m^2 for oil M1, 307 MW/m^2 for oil M2, 446 MW/m^2 for oil EAL1, and 355 MW/m^2 for oil EAL2.

In Figs. 3 and 4, a good repeatability can be observed for the scuffing capacity and friction results that approved the accuracy of the test. It is noteworthy that the bath oil temperature variation was less than 1 °C

Table 4
Test parameters.

	Running-in	Extra running-in	Test stage	Rest stage
Sliding speed	100 mm/s	300 mm/s-500 mm/s	600 mm/s-4000 mm/s for 20 N and 50 load steps 600 mm/s-6000 mm/s for 70 N	0
Rolling speed	40 mm/s	100 mm/s	100 mm/s	0
Temperature	120 °C	120 °C	120 °C	120 °C
Load	10 N (Pmax: 1.56 GPa)	20 N - Pmax: 1.97 GPa, Pmean: 1.31 GPa 50 N - Pmax: 2.67 GPa, Pmean: 1.79 GPa 75 N - Pmax: 3.06 GPa, Pmean: 2.05 GPa	20 N - Pmax: 1.97 GPa, Pmean: 1.31 GPa 50 N - Pmax: 2.67 GPa, Pmean: 1.79 GPa 75 N - Pmax: 3.06 GPa, Pmean: 2.05 GPa	0
Duration	600 s	30 s per step	30 s per step	30 s

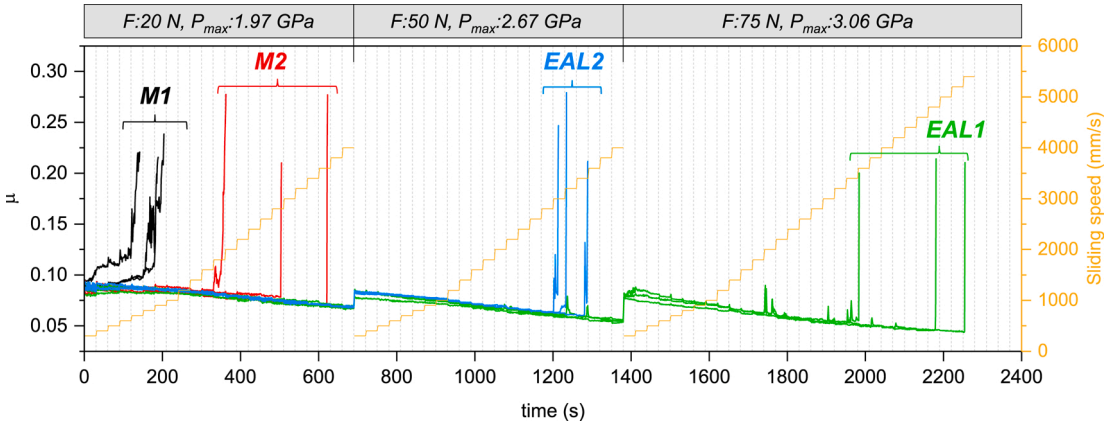

Fig. 3. The friction coefficient, sliding speed and load during the scuffing test of oils.

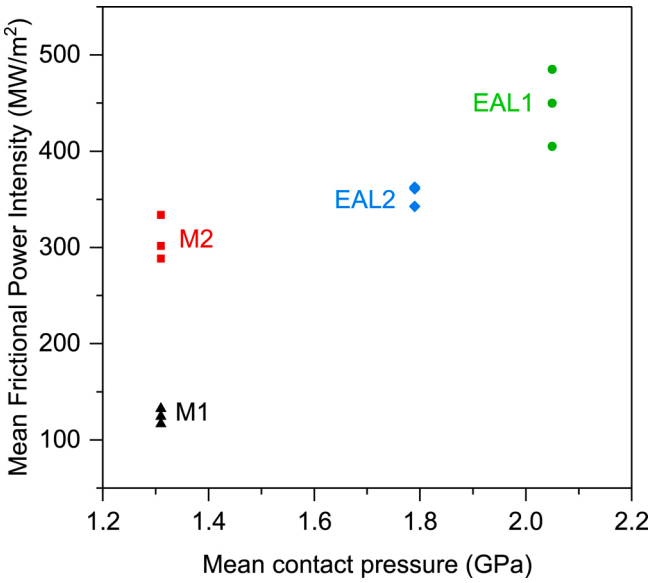

Fig. 4. Mean frictional power intensity at scuffing against mean contact pressure for the tested oils.

Table 5
Estimated dynamic viscosity, pressure-viscosity coefficient and EHL film thickness of the lubricants at the test temperature.

	η @120 °C (mPa s)	α @120 °C (1/GPa)	h_{min} @20 N (nm)	h_{min} @50 N (nm)	h_{min} @75 N (nm)
M1	7.12	12.58	2.35	2.2	2.14
M2	7.065	12.6	2.34	2.19	2.13
EAL1	10.62	8.94	2.61	2.44	2.37
EAL2	9.868	8.88	2.48	2.32	2.25

during the test, and no oil temperature rise was observed before scuffing. This means that the generated heat does not result in the oil temperature increase. On the other hand, the rest steps let the generated heat dissipates and the heating control system keeps the oil temperature constant.

The benefit of low traction (friction) oil on scuffing has been discussed in Ref. [42]. In Fig. 3, the friction is not considerably different for the oils, because they are in a boundary lubrication regime, and in this regime, the oil traction plays a minor role. However, the same oils used in the current study were also used in other studies [43,44], and EAL1 and EAL2 showed considerably lower traction in EHL and mixed regimes.

As EHL film thickness plays a very important role in scuffing, thus the minimum EHL film thickness was calculated using Hamrock and Dowson's formula (Eqs. (4) and (5)) [45].

$$h_{min} = 3.63R_x\left(\frac{U_e\eta_0}{E^*R_x}\right)^{0.68}(\alpha E^*)^{0.49}\left(\frac{F}{E^*R_x^2}\right)^{-0.073}\left(1-e^{-0.68k}\right) \quad (4)$$

$$k = 1.0339\left(\frac{R_y}{R_x}\right)^{0.636} \quad (5)$$

where R_x and R_y are the radius of curvature in the x and y direction (m), U_e is the entrainment speed (m/s), η_0 is the dynamic viscosity of the lubricant (Pa.s) at test temperature, E^* is the reduced Young's Modulus (Pa), α is the pressure-viscosity coefficient (Pa^{-1}) at test temperature, F is the applied load (N). Pressure-viscosity coefficient and dynamic viscosity at the test temperature (120 °C) were estimated using a method presented in Ref. [32]. The results are shown in Table 5.

With the film thickness in Table 5 and the surface roughness in Table 1, it is evident that the system is operating under boundary lubrication regime. However, the EALs show higher EHL film thickness in Table 5. Comparing the oils' pressure-viscosity coefficient and dynamic viscosity illustrates that the higher EHL film thickness of EALs is due to their higher dynamic viscosity at the test temperature. The higher viscosity index of EALs helps them to have higher viscosity in high temperature which is beneficial for preventing the failures associated with high temperature. It is noticeable that in Eq. (4), the thermal effect is not considered for calculating the EHL film thickness. Considering the fact that EALs (mainly ester or PAO molecules) have bigger thermal conductivity [46], the difference between the EHL film thickness of EALs and mineral oil can be even higher.

In addition to the EHL film, tribofilm also plays an important role in preventing scuffing failure. Using the SLIM technique, the tribofilm evolution was captured at load stage of F = 20 N, and three sliding speeds of 2200 mm/s, 2800 mm/s and 3400 mm/s. These tribofilm images can be observed in Fig. 5 (the tribofilm for M1 is not shown, because its scuffing happened at much lower speeds). The tribofilm is the dark area along the sliding direction. The exact thickness can be measured using the technique explained in Ref. [43], however, the images are more informative in this case that the tribofilm is not uniformly covering the surface. A darker tribofilm means a higher thickness, and it can be quickly observed that the tribofilm thickness of EALs is higher than that of M2. It was surprising because the mineral oils do not have the restriction of EALs for using environmentally acceptable additives,

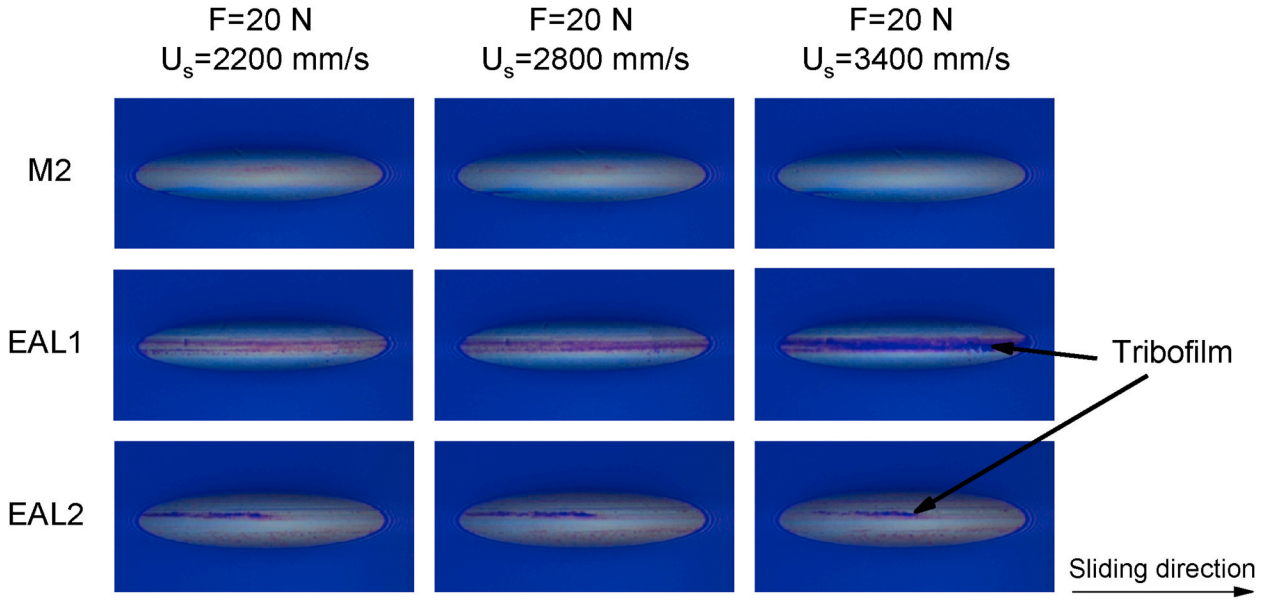

Fig. 5. Tribofilm thickness of oils M2, EAL1 and EAL2 at F = 20 N, and sliding speeds of 2200 mm/s, 2800 mm/s and 3400 mm/s.

thus they usually contain additives with superior performance [32]. From Table 3, it can be seen that M2 contains a considerable amount of sulfuric EP additives. However, these additives do not compensate for the effect of its lower EHL film. With this hypothesis that M2 contains more reactive additives, it can be said that the lower EHL film thickness in this oil results in fast removal of the tribofilm, and prevention of a thick tribofilm formation. This was the case for M1 also, which contained highly reactive additives [43] but could not form a thick tribofilm in this scuffing test due to its low EHL film thickness. In contrast, for the case of EAL1 and EAL2, the higher EHL film thickness enables the tribofilm to be formed. Therefore, these findings imply that a minimum EHL film thickness is always required for tribofilm formation. The EALs showed superior scuffing capacity that is mainly due to their higher viscosity index that allows them to form a thick EHL film. This EHL film not only increases their ability to separate the sliding bodies but also provides the proper condition for a thick tribofilm formation.

It is noticeable to say that except for the case of M1, all the other oil had an FZG scuffing capacity of 12+ according to the manufacturer datasheet. However, using the currently developed technique, the scuffing capacity of the oils is ranked as EAL1>EAL2>M2>M1. Although the test method is similar to what was developed in Refs. [29, 30], the adjustment of parameters and combination of sliding speed-step and load-step enables this test method to evaluate the industrial oil with high scuffing capacity, and distinguish between the scuffing capacity of oils with the same FZG results. However, this does not mean that this test can replace the FZG scuffing test method. FZG test has the advantage of representing real component conditions including impact, pressure and speed variations, as well as bigger curvature, lower wear rate, and higher roughness.

3.2. The relation between tribofilm and scuffing

Figs. 6 and 7 show the SLIM images for the oil EAL1 (rest stage time is not included). In these graphs, only the SLIM images are shown that

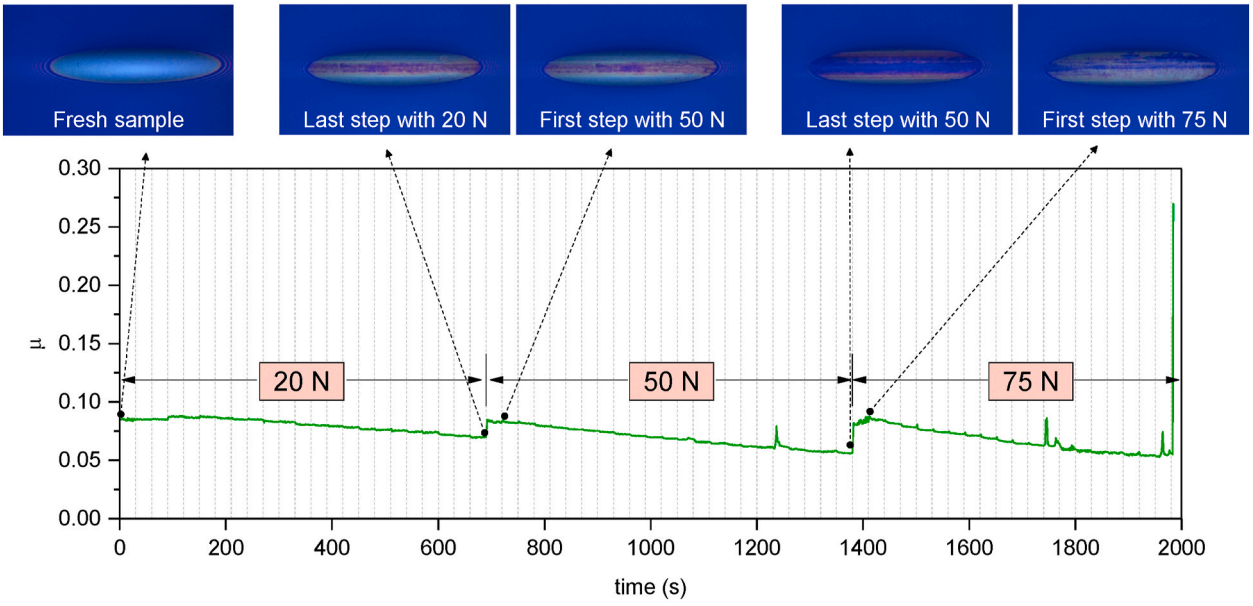

Fig. 6. SLIM images for the scuffing test of EAL1, captured before and after changing the load.

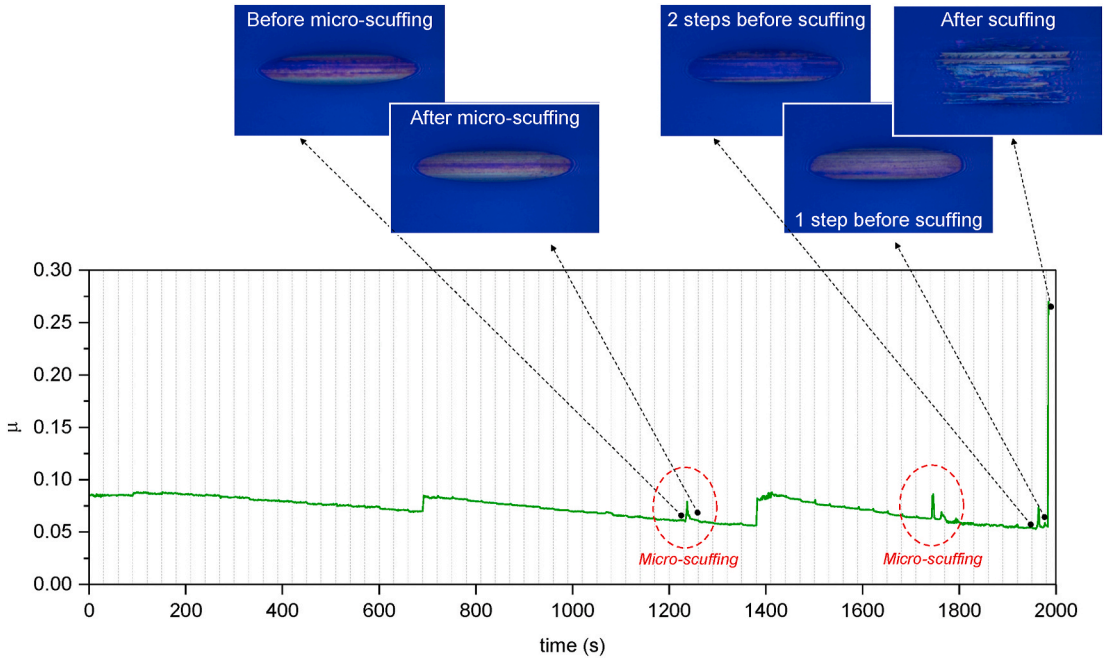

Fig. 7. SLIM images for the scuffing test of EAL1, captured before and after a micro-scuffing and the scuffing.

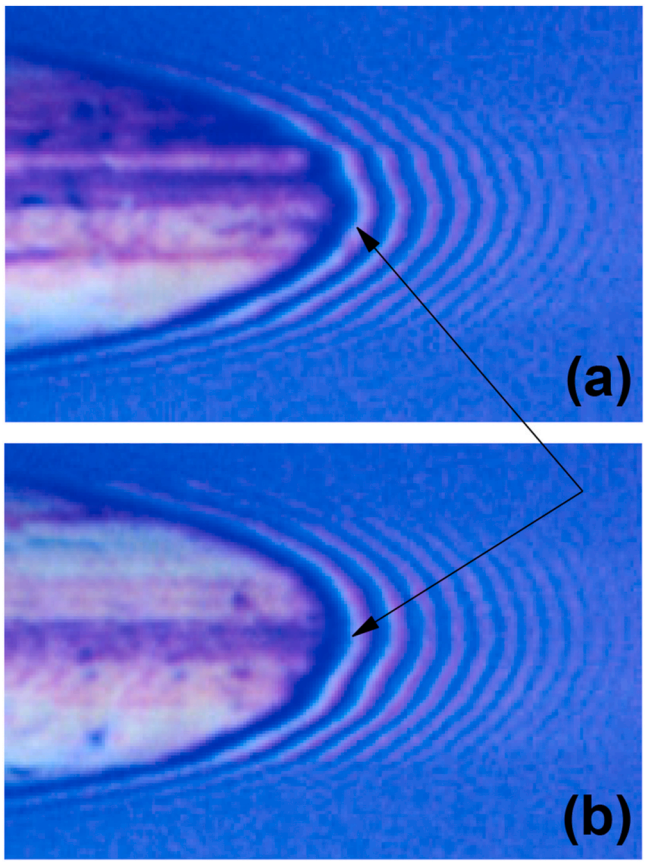

Fig. 8. Geometrical change of the barrel after micro-scuffing: (a) Before micro-scuffing, (b) After micro-scuffing.

contain specific characteristics in this scuffing test. In Fig. 6, the SLIM images are shown just before and after changing the load. It can be seen that after increasing the load, the tribofilm thickness decreased. This is more visible for the case of changing from 50 N to 75 N load. The removal of tribofilm leads to direct contact between the metallic surfaces, but it did not lead to scuffing in this test as the sliding velocity was very low after increasing the load. This is the reason that extra running-in stages were added before each load stage (Fig. 2) to give enough time for the tribofilm to be formed again. This is a very important point that must be carefully inspected in scuffing tests based on step loads (for example FZG scuffing test). In the step-load scuffing tests, by increasing the load, a fresh area of the sample with unworn asperities comes into the contact that is not protected by a tribofilm. In addition, the previously formed tribofilm is also removed. Thus, it can lead to premature scuffing. The current developed test plan prevents this kind of failure by a low sliding speed at the start of the load steps that is a kind of short running-in period. Therefore, it is recommended to have a short running-in with the same load (as the load step) and low sliding speed in a scuffing test. This is an important point to know for the other applications in which overload is critical in scuffing. In such applications, a low-speed running-in with high loads helps the formation of tribofilm over the unprotected contact area of lubricated components. The SLIM images showed that in high load conditions, the tribofilm can cover the contact area in less than 60 s.

In Fig. 7, the SLIM images of oil EAL1 are presented before and after scuffing, and before and after a micro-scuffing. The "micro-scuffing" refers to local scuffing that does not propagate to the whole surfaces, and appears as a sudden rise and quick fall of friction coefficient [4,17,29,39,47–49]. Regarding micro-scuffing, different studies report microstructural change and instantaneous plastic flow accompanied by a temperature rise [17,18,49]. However, the temperature rise and wear of micro-scuffing are not considerable compared to those of the final scuffing [49]. Micro-scuffing appears when the plastic flow of the material does not lead to a total failure, and a "healing" or "quenching" process prevents the scuffing propagation [17,39].

The healing process is attributed to a quick dissipation of heat [19] and reduced normal pressure due to the increased contact area [49]. In the current test, Fig. 7 shows the tribofilm removal after the micro-scuffing. Also, the increasing contact area was detected after the micro-scuffing that is hard to observe in Fig. 7. Thus, the SLIM images were magnified in Fig. 8 to distinguish between the contact area of the barrel before and after the micro-scuffing. In Fig. 8, the widened contact area signifies a small change in the barrel's edge radius and the removal of a very thin layer from the specimen.

When micro-scuffing happens, a thin layer of material experiences plastic deformation and results in some heat generation. This is the layer in which the rate of thermal softening exceeds the rate of work hardening. After that, a new layer with new mechanical properties comes into contact. If the thermal softening is still so high that can remove that surface, the scuffing propagates [17,18]. In this stage, if the lubricant transfers enough amount of heat, and the tribofilm is recovered quickly, then the healing happens. From Fig. 3, it was observed that the healing process and micro-scuffing of EAL1 happened at the same sliding speeds in which EAL2 experienced scuffing (Fig. 3). This shows that EAL1 had a higher scuffing healing ability. Accordingly, the higher healing ability of EAL1 is attributed to its superior EHL film (Table 5) and tribofilm (Fig. 5). While EAL1 and EAL2 are both from the same oil type, and viscosity class, they show different scuffing capacities. This indicates that minor changes in the lubricant formulation can result in healing of scuffing, and better scuffing capacity of the oil. One probable reason for such a case can be the higher phosphorous content of EAL 1 that leads to a thicker and more reactive tribofilm (Fig. 5) and a better micro-scuffing healing.

Regarding the final scuffing of EAL1 in Fig. 7, a micro-scuffing was also observed just prior to the final friction rise. Before that micro-scuffing, a thick tribofilm was protecting the surface, but after that micro-scuffing, the tribofilm thickness was very thin that provided the condition for the final scuffing. Although after that micro-scuffing the surface was slightly widened, it was not enough to postpone the scuffing. Although the tribofilm-friction graph is shown only for EAL1, the link between the micro-scuffing, scuffing and tribofilm can be generalized for the other tested oils.

3.3. *Surface profile before, during and after the scuffing test*

To further study the surface modification of the samples, their surface profile was captured by an Alicona InfiniteFocus G5 optical profilometry system. Fig. 9 shows the barrel surface and profile before, during and after the test. Compared to the visible scuffing scar in Fig. 9 (c), no considerable deformation can be observed after the load stage of 50 N (Fig. 9 (b)). However, as it was discussed about SLIM images in section 3.2, micro-scuffing results in small geometrical modifications. This surface modification was hard to measure by Alicona optical profilometer.

The disc was also observed after the 50 N load step, and after scuffing (Fig. 10). Again, no considerable geometrical change was observed after the load stage of 50 N on the disc. This approves the successful implementation of this test method by eliminating the wear adverse effect. In Fig. 10 (b), the wear grooves in the sliding direction show severe cutting happened due to adhesion of the metal surfaces.

4. Conclusion

The objective of this work was to develop a fast contra-rotating method to evaluate the scuffing capacity of fully formulated EALs. The developed test method used a barrel-on-disc specimen setup to reach higher contact pressures up to 3.06 GPa, and employing scuffing steps

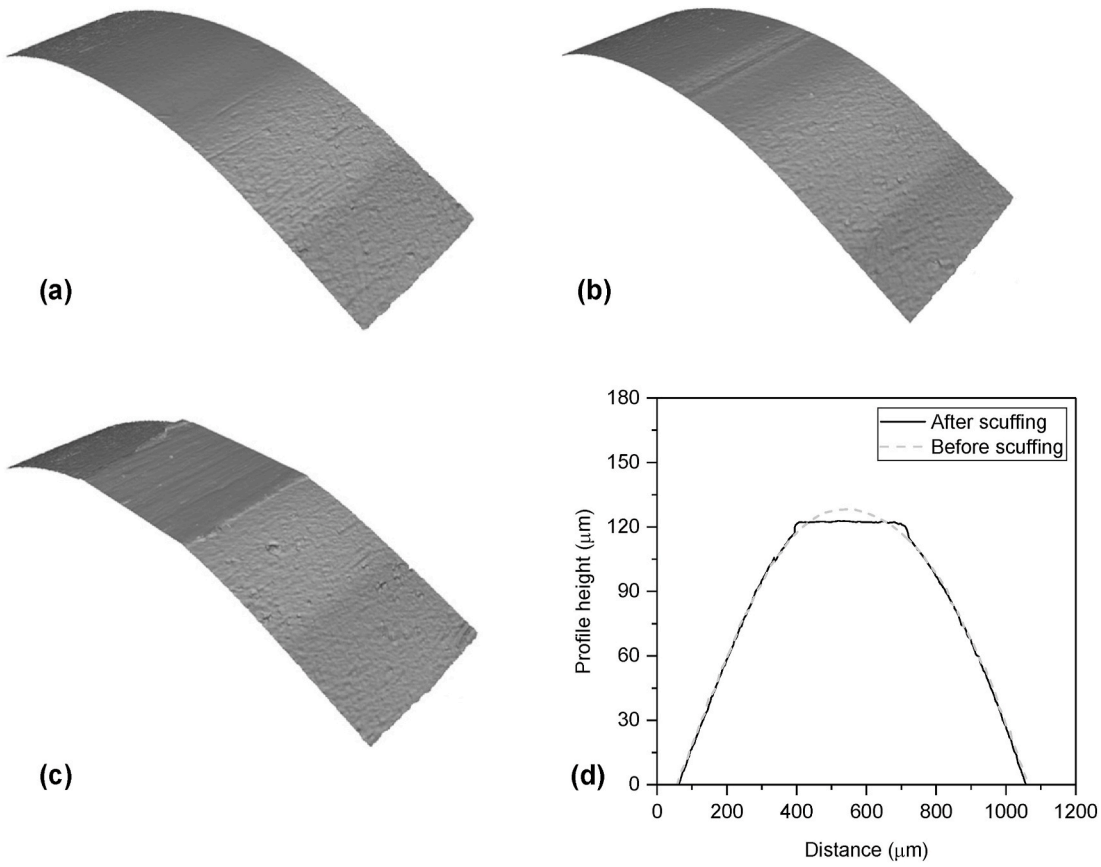

Fig. 9. Example images of the barrel edge for the oils EAL1: (a) new barrel (b) after the load stage 50 N (no scuffing yet) (c) after scuffing (d) barrel profile before and after scuffing.

combining sliding speed steps and load steps. Furthermore, the tribofilm evolution was captured by the SLIM technique to illustrate the interaction between the EHL film and tribofilm. Two industrial EALs formulated for gears and two fully formulated mineral oils were evaluated with this new scuffing test method. The results showed that:

- Careful selection of running-in parameters is very important in achieving reliable scuffing results. In addition to a primary running-in with low load and low speed, a short running-in is recommended before each load step. This short running-in must have the same load as the test to enhance tribofilm coverage on the unprotected areas. Also, this short running-in must have a low sliding speed and short duration to prevent unwanted wear.
- The advantages of the developed test are:
  - o Differentiating between the scuffing capacity of the oils which had similar FZG scuffing capacity in their datasheet.
  - o Providing high sliding speeds while maintaining a low entrainment speed so that high-performance oils can be tested successfully.
  - o Minimizing the wear before scuffing by using rolling–sliding conditions.
- The scuffing is identified by a sudden unrecoverable increase of friction coefficient resulting in a high wear rate and destruction of the surface. Micro-scuffing is identified by a temporary and recoverable friction rise that results in the removal of tribofilm and plastic deformation in several material layers.
- The healing of micro-scuffing happens by small changes in the contact area and accordingly alternation of the normal pressure distribution. In addition, EHL and tribofilm play a significant role in micro-scuffing healing. Small variations in the lubricant formulation have a significant effect on the healing of micro-scuffing.
- After increasing the load in a scuffing test, the thickness of tribofilm decreases that is more evident at high loads. At the high loads, the tribofilm can be recovered if the sliding speed is low. However, at such high loads, if the sliding speed is not low, the increased load brings the fresh unprotected area into the contact and results in unwanted scuffing. Thus, it is recommended that the load increase is accompanied by a low speed to prevent scuffing.
- The tested EALs showed superior scuffing capacity than mineral oils. This was mainly due to their higher viscosity index that allowed them to form a thick EHL film at high temperatures.
- The tested EALs formed a thicker tribofilm in scuffing tests despite having the restriction of using only environmentally acceptable additives. A minimum EHL film thickness is always required for tribofilm formation.

CRediT authorship contribution statement

Reza Bayat: Conceptualization, Methodology, Software, Validation, Formal analysis, Investigation, Resources, Data curation, Writing – original draft, Writing – review & editing, Visualization. **Arto Lehtovaara:** Conceptualization, Writing – review & editing, Supervision, Project administration.

Declaration of competing interest

The authors declare that they have no known competing financial interests or personal relationships that could have appeared to influence the work reported in this paper.

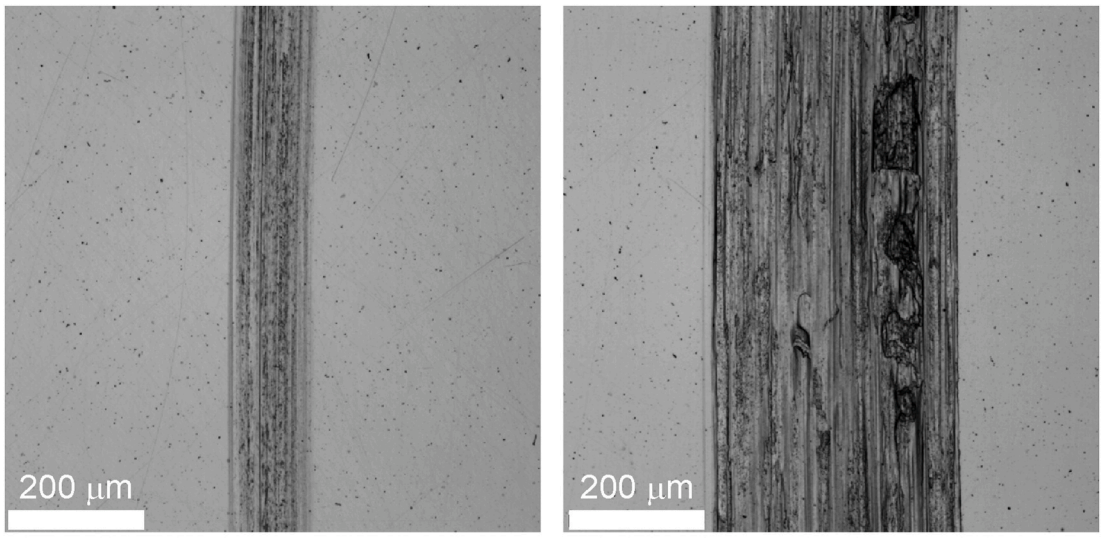

Fig. 10. Example images of the disc for the oils EAL1: (a) after the load stage 50 N (no scuffing yet) (b) after scuffing.

Acknowledgments

We gratefully acknowledge the financial support from Tampere University graduate school.

References

[1] Saeidi F, Shevchik SA, Wasmer K. Automatic detection of scuffing using acoustic emission. Tribol Int 2016;94:112–7. https://doi.org/10.1016/j.triboint.2015.08.021.
[2] Savolainen M, Lehtovaara A. An experimental approach for investigating scuffing initiation due to overload cycles with a twin-disc test device. Tribol Int 2017;109:311–8. https://doi.org/10.1016/J.TRIBOINT.2017.01.005.
[3] Schipper DJ, De Gee AWJ. Lubrication modes and the IRG transition diagram. Lubric Sci 1995;8:27–35. https://doi.org/10.1002/ls.3010080104.
[4] Yagi K, Izumi T, Koyamachi J, Sanda S, Yamaguchi S, Satio K, et al. In situ observation of crystal grain orientation during scuffing process of steel surface using synchrotron X-ray diffraction. Tribol Lett 2020;68:115. https://doi.org/10.1007/s11249-020-01357-y.
[5] Christensen H. Failure by collapse of hydrodynamic oil films. Wear 1972;22:359–66. https://doi.org/10.1016/0043-1648(72)90394-8.
[6] Höhn BR, Michaelis K. Influence of oil temperature on gear failures. Tribol Int 2004;37:103–9. https://doi.org/10.1016/S0301-679X(03)00047-1. Elsevier.
[7] Li S, Kahraman A, Anderson N, Wedeven LD. A model to predict scuffing failures of a ball-on-disk contact. Tribol Int 2013;60:233–45. https://doi.org/10.1016/j.triboint.2012.11.007.
[8] Castro J, Seabra J. Influence of mass temperature on gear scuffing. Tribol Int 2018;119:27–37. https://doi.org/10.1016/j.triboint.2017.10.032.
[9] Yagi K, Ebisu Y, Sugimura J, Kajita S, Ohmori T, Suzuki A. In situ observation of wear process before and during scuffing in sliding contact. Tribol Lett 2011;43:361–8. https://doi.org/10.1007/s11249-011-9817-3.
[10] Batchelor AW, Stachowiak GW. Model of scuffing based on the vulnerability of an elastohydrodynamic oil film to chemical degradation catalyzed by the contacting surfaces. Tribol Lett 1995;1:349–65. https://doi.org/10.1007/BF00174259.
[11] Wojciechowski L, Kubiak KJ, Mathia TG. Roughness and wettability of surfaces in boundary lubricated scuffing wear. Tribol Int 2016;93:593–601. https://doi.org/10.1016/j.triboint.2015.04.013.
[12] Spikes H, Jie Z. History, origins and prediction of elastohydrodynamic friction. Tribol Lett 2014;56:1–25. https://doi.org/10.1007/s11249-014-0396-y.
[13] Spikes HA, Cameron A. Scuffing as a desorption process—an explanation of the borsoff effect. ASLE Trans 1974;17:92–6. https://doi.org/10.1080/05698197408981442.
[14] Blok H. The flash temperature concept. Wear 1963;6:483–94. https://doi.org/10.1016/0043-1648(63)90283-7.
[15] Dyson A. The failure of elastohydrodynamic lubrication of circumferentially ground discs. Proc Inst Mech Eng 1976;190:699–711. https://doi.org/10.1243/pime_proc_1976_190_074_02.
[16] Cheng HS, Dyson A. Elastohydrodynamic lubrication of circumferentially–ground rough disks. ASLE Trans 1978;21:25–40. https://doi.org/10.1080/05698197808982858.
[17] Hershberger J, Ajayi OO, Zhang J, Yoon H, Fenske GR. Evidence of scuffing initiation by adiabatic shear instability. Wear 2005;258:1471–8. https://doi.org/10.1016/j.wear.2004.10.010.
[18] Ajayi OO, Hersberger JG, Zhang J, Yoon H, Fenske GR. Microstructural evolution during scuffing of hardened 4340 steel - implication for scuffing mechanism. Tribol Int 2005;38:277–82. https://doi.org/10.1016/j.triboint.2004.08.011. Elsevier.
[19] Ajayi OO, Lorenzo-Martin C, Erck RA, Fenske GR. Scuffing mechanism of near-surface material during lubricated severe sliding contact. Wear 2011;271:1750–3. https://doi.org/10.1016/j.wear.2010.12.086.
[20] Ajayi OO, Lorenzo-Martin C, Erck RA, Fenske GR. Analytical predictive modeling of scuffing initiation in metallic materials in sliding contact. Wear 2013;301:57–61. https://doi.org/10.1016/j.wear.2012.12.054.
[21] Zhang C, Peng B, Gu L, Wang T, Wang L. A scuffing criterion of steels based on the friction-induced adiabatic shear instability. Tribol Int 2020;148:106340. https://doi.org/10.1016/j.triboint.2020.106340.
[22] American Society for Testing. Materials: ASTM D1947 test method for, load-carrying capacity of petroleum oil and synthetic fluid gear lubricants. 1993.
[23] Energy Institute (formerly Institute of Petroleum, IP): IP 166: 77(R1992) Determination of load-carrying capacity of lubricants—IAE gear machine method.
[24] ISO: ISO 14635 Part 1: gears-FZG test procedures-Part 1: FZG test method A/8,3/90 for scuffing 1736 load-carrying capacity of oils. 2000.
[25] Castro J, Seabra J. Global and local analysis of gear scuffing tests using a mixed film lubrication model. Tribol Int 2008;41:244–55. https://doi.org/10.1016/j.triboint.2007.07.005.
[26] ASTM D2782: Standard test method for measurement of extreme-pressure properties of lubricating grease (Timken Method).
[27] ASTM D2596: Standard test method for measurement of extreme-pressure properties of lubricating grease (Four-Ball Method).
[28] Savolainen M, Lehtovaara A. An experimental investigation of scuffing initiation due to axial displacement in a rolling/sliding contact. Tribol Int 2018;119:688–97. https://doi.org/10.1016/j.triboint.2017.12.007.
[29] Peng B, Spikes H, Kadiric A. The development and application of a scuffing test based on contra-rotation. Tribol Lett 2019;67:37. https://doi.org/10.1007/s11249-019-1149-8.
[30] Ingram M, Hamer C, Spikes HA. A new scuffing test using contra-rotation. Wear 2015;328–329:229–40. https://doi.org/10.1016/j.wear.2015.01.080.
[31] Vrcek A, Hultqvist T, Baubet Y, Björling M, Marklund P, Larsson R. Micro-pitting and wear assessment of engine oils operating under boundary lubrication conditions. Tribol Int 2019;129:338–46. https://doi.org/10.1016/j.triboint.2018.08.032.
[32] Brandão JA, Meheux M, Ville F, Seabra JHO, Castro J. Comparative overview of five gear oils in mixed and boundary film lubrication. Tribol Int 2012;47:50–61. https://doi.org/10.1016/j.triboint.2011.10.007.
[33] Brandão JA, Meheux M, Seabra JHO, Ville F, Castro MJD. Traction curves and rheological parameters of fully formulated gear oils. Proc Inst Mech Eng Part J J Eng Tribol 2011;225:577–93. https://doi.org/10.1177/1350650111405111.
[34] Martins R, Seabra J, Brito A, Seyfert C, Luther R, Igartua A. Friction coefficient in FZG gears lubricated with industrial gear oils: biodegradable ester vs. mineral oil. Tribol Int 2006;39:512–21. https://doi.org/10.1016/J.TRIBOINT.2005.03.021.
[35] Hammami M, Rodrigues N, Fernandes C, Martins R, Seabra J, Abbes MS, et al. Axle gear oils: friction, wear and tribofilm generation under boundary lubrication regime. Tribol Int 2017;114:88–108. https://doi.org/10.1016/J.TRIBOINT.2017.04.018.

[36] Rycerz P, Kadiric A. The influence of slide–roll ratio on the extent of micropitting damage in rolling–sliding contacts pertinent to gear applications. Tribol Lett 2019; 67:1–20. https://doi.org/10.1007/s11249-019-1174-7.
[37] Bergseth E, Zhu Y, Söderberg A. Study of surface roughness on friction in rolling/sliding contacts: ball-on-disc versus twin-disc. Tribol Lett 2020;68:1–15. https://doi.org/10.1007/s11249-020-01310-z.
[38] Gould B, Demas NG, Pollard G, Rydel JJ, Ingram M, Greco AC. The effect of lubricant composition on white etching crack failures. Tribol Lett 2019;67:1–24. https://doi.org/10.1007/s11249-018-1106-y.
[39] Ludema KC. A review of scuffing and running-in of lubricated surfaces, with asperities and oxides in perspective. Wear 1984;100:315–31. https://doi.org/10.1016/0043-1648(84)90019-X.
[40] Fujita H, Spikes HA. Study of zinc dialkyldithiophosphate antiwear film formation and removal processes, part II: kinetic model. Tribol Trans 2005;48:567–75. https://doi.org/10.1080/05698190500385187.
[41] Matveevsky RM. The critical temperature of oil with point and line contact machines. J Basic Eng 1965;87:754–9. https://doi.org/10.1115/1.3650672.
[42] Jackson A, Webster MN, Enthoven JC. The effect of lubricant traction on scuffing. Tribol Trans 1994;37:387–95. https://doi.org/10.1080/10402009408983307.
[43] Bayat R, Lehtovaara A. EHL/mixed transition of fully formulated environmentally acceptable gear oils. Tribol Int 2020;146. https://doi.org/10.1016/j.triboint.2020.106158.
[44] Bayat R, Lehtovaara A. Friction and temperature mapping of environmentally acceptable gear oils. Tribol Fin J Tribol 2020;37:4–12. https://doi.org/10.30678/fjt.96048.
[45] Hamrock BJ, Dowson D. Minimum film thickness in elliptical contacts for different regimes of fluid-film lubrication. 1978. Cleveland, Ohio.
[46] Larsson R, Andersson O. Lubricant thermal conductivity and heat capacity under high pressure. Proc Inst Mech Eng Part J J Eng Tribol 2000;214:337–42. https://doi.org/10.1243/1350650001543223.
[47] Yoon H, Zhang J, Kelley F. Scuffing characteristics of sae 50b38 steel under lubricated conditions. Tribol Trans 2002;45:246–52. https://doi.org/10.1080/10402000208982547.
[48] Matsuzaki Y, Yagi K, Sugimura J. In situ observation of heat generation behaviour on steel surface during scuffing process. Tribol Lett 2018;66:142. https://doi.org/10.1007/s11249-018-1095-x.
[49] Yagi K, Kajita S, Izumi T, Koyamachi J, Tohyama M, Saito K, et al. Simultaneous synchrotron X-ray diffraction, near-infrared, and visible in situ observation of scuffing process of steel in sliding contact. Tribol Lett 2016;61:1–16. https://doi.org/10.1007/s11249-015-0636-9.